

## Article

# Most Southern Scots Pine Populations Are Locally Adapted to Drought for Tree Height Growth

Natalia Vizcaíno-Palomar <sup>1,\*</sup> , Noelia González-Muñoz <sup>1</sup>, Santiago C. González-Martínez <sup>1</sup> , Ricardo Alía <sup>2</sup>  and Marta Benito Garzón <sup>1</sup> 

<sup>1</sup> BIOGECO, INRA, Univ. Bordeaux, 33615 Pessac, France

<sup>2</sup> INIA, Forest Research Centre & iuFOR UVa-INIA, Ctra La Coruña km 7.5, 28040 Madrid, Spain

\* Correspondence: natalia.vizcaino.palomar@gmail.com

Received: 12 June 2019; Accepted: 29 June 2019; Published: 2 July 2019



**Abstract:** Most populations of Scots pine in Spain are locally adapted to drought, with only a few populations at the southernmost part of the distribution range showing maladaptations to the current climate. Increasing tree heights are predicted for most of the studied populations by the year 2070, under the RCP 8.5 scenario. These results are probably linked to the capacity of this species to acclimatize to new climates. The impact of climate change on tree growth depends on many processes, including the capacity of individuals to respond to changes in the environment. Pines are often locally adapted to their environments, leading to differences among populations. Generally, populations at the margins of the species' ranges show lower performances in fitness-related traits than core populations. Therefore, under expected changes in climate, populations at the southern part of the species' ranges could be at a higher risk of maladaptation. Here, we hypothesize that southern Scots pine populations are locally adapted to current climate, and that expected changes in climate may lead to a decrease in tree performance. We used Scots pine tree height growth data from 15-year-old individuals, measured in six common gardens in Spain, where plants from 16 Spanish provenances had been planted. We analyzed tree height growth, accounting for the climate of the planting sites, and the climate of the original population to assess local adaptation, using linear mixed-effect models. We found that: (1) drought drove differences among populations in tree height growth; (2) most populations were locally adapted to drought; (3) tree height was predicted to increase for most of the studied populations by the year 2070 (a concentration of RCP 8.5). Most populations of Scots pine in Spain were locally adapted to drought. This result suggests that marginal populations, despite inhabiting limiting environments, can be adapted to the local current conditions. In addition, the local adaptation and acclimation capacity of populations can help margin populations to keep pace with climate change. Our results highlight the importance of analyzing, case-by-case, populations' capacities to cope with climate change.

**Keywords:** climate change; gene flow; local adaptation; maladaptation; mixed-models; phenotypic plasticity; phenotypic variation

## 1. Introduction

The impact of climate change on tree growth is complex, because it depends on many biotic and abiotic processes, and hence, it remains difficult to predict. Northern and western European forests may benefit from warmer temperatures, with positive effects on tree growth [1–4], but at the same time, tree mortality has increased during the last years [5]. Contrarily, southern and eastern European forests can experience reductions in their growth rates as a consequence of more frequent and intense episodes of drought [1,6]. In natural populations, tree growth strongly depends on climate and stand structure, and on processes related to competition and facilitation among individuals. This complexity

varies across geographical scales [4,7,8]. Moreover, tree height growth, related to biomass, and thus, to reproduction, is an important component of fitness with moderate heritability [9] that can show population-level differentiation as a result of local adaptation [10,11]. Likewise, tree height growth can express plasticity (i.e., acclimation) as a result of rapid changes in the environment [12,13].

In the past, natural selection driven by climate may have led to differences among populations in fitness-related traits [10,14]. As a result, tree populations show moderate to strong local adaptation, despite having high levels of gene flow [15]. A locally adapted population is expected to reach its optimum performance (i.e., maximum performance) and outperform non-local populations at its local habitat [16]. However, genetic and demographic processes are different across species' ranges, leading to remarkable differences between the core and margin populations [17]. Generally, populations' performances are lower in the margin populations than in the core populations, although this pattern is trait-dependent [12,18]. For instance, tree growth generally declines towards the margins of species' ranges [19,20], although it can be compensated by trade-offs with other fitness related traits [21–23]. Among the different processes that influence trait patterns across species' ranges, genetic adaptation in margin tree populations is particularly important in the context of climate change.

Common garden experiments (provenance tests) offer an ideal framework to evaluate local adaptation [16,24]. The phenotypic data measured in these experimental designs allow one to estimate populations' responses to different environments (i.e., reaction norms or plastic responses) and the effect that is attributable to genetic processes. Likewise, common gardens can be used to define a locally adapted population when the local population shows a higher level of fitness (measured from fitness-related traits) than the non-local population when measured in its own habitat [16].

Scots pine (*Pinus sylvestris* L.) is one of the most widely distributed species in the world [25], with a natural range from beyond the Arctic Circle in Scandinavia to southern Spain, and from western Scotland to the Okhotsk Sea in eastern Siberia. In general, Scots pine tree growth is limited by high temperatures found in the southern part of the range and at low elevations [26], cold temperatures at the northern part of the range and at high elevations [26,27], and by the combination of photoperiod and cold hardiness at the northernmost part of the range [28]. The southern range of Scots pine is reached in Spain. Here, Scots pine presents a fragmented distribution, with high genetic differentiation between populations [29–31]. The Spanish populations are mostly found in mountainous areas, growing under the influence of continental or Mediterranean climates, which are characterized by dry summers and cold winters inland, and by mild winters in coastal areas [32], respectively. These marginal populations can be more vulnerable as they inhabit less favorable habitats, where water availability becomes the main constraint of forest growth [33], compromising natural regeneration [34]. Recent warming trends in the climate have exacerbated drought stress, and have negatively impacted tree growth, probably due to an increase in respiration rates and a lower carbon uptake [35,36]. However, these studies have overlooked population-level variation with regard to adaptation and acclimation potential. Previous models, including local adaptation and phenotypic plasticity data, predicted a greater habitat suitability for Scots pine in Spain than classic species distribution models, based exclusively on species occurrence [30], suggesting that these processes are crucial for assessing future predictions of tree height across the species range. However, the extent to which southern Scots pine populations are at a high risk of maladaptation under expected climate change is unclear.

Here, we hypothesize that southern Scots pine populations are locally adapted to the current climate, and that expected changes in climate may lead to a decrease in tree performance. To evaluate our hypothesis, we analyze Scots pine tree height growth data as a proxy of fitness [37,38], from 15-year-old individuals that were measured in a network of common gardens planted in Spain, the southern part of the species' range. This network gathers six planting sites, in which plants of 16 Spanish provenances had been planted. We define the following objectives: (1) we identify the main climatic drivers shaping among-population differentiation and phenotypic plasticity, (2) we assess if local populations outperform non-local populations at their local environments, and (iii) we predict

tree height growth, accounting for the genetic effect of the populations and the phenotypic plasticity, in the southern range of the species under future climates, to assess the impact of climate change.

## 2. Material and Methods

### 2.1. Phenotypic Data and Common Gardens

We used the tree height growth data of Scots pine (*P. sylvestris*) from 15-year-old plants measured in six planting sites established in Spain, the southern range of the species (Figure A1). Sixteen genetically distinct Spanish populations [30,31,39] that cover the species distribution in Spain were planted in each planting site (Figure A1). The seeds for population seedlots were collected during the years 1988 and 1989 [39,40]. A seedlot was composed by mixing the seeds collected in natural populations from at least 25 mother trees, with a 50-m separation distance between each individual, to avoid interbreeding [41]. In 1991, two-year-old plantlets originating from the seedlots were planted in the planting sites, following a randomized complete block design, with four blocks and a 16-tree square plot for each population, planted at a 2.5 × 2.5 m spacing.

### 2.2. Climate Data

We used two sources of gridded climate data for the present and future conditions:

(1) We used the Gonzalo-Jiménez [42] Spanish climatic model—the average climate was calculated for the period between 1961 and 1999—covering Spain at 30 arc sec resolution (~1 × 1 km), to calibrate our models. We used a total of 51 temperature and precipitation-related climate variables to accurately assess the main climatic drivers promoting among-population differentiation and plasticity (Table 1). We named the climatic variables of the planting site and the population origin *\_s* or *\_p*, respectively (e.g., AHM<sub>s</sub> and AHM<sub>p</sub> for the annual heat-moisture index of the planting site or at the population origin, respectively).

**Table 1.** Temperature- and precipitation-related climate variables considered in the present study.

	Monthly temperature (T, °C)	T.jan, T.feb, T.mar, T.apr, T.may, T.jun, T.jul, T.ago, T.sep, T.oct, T.nov, T.dec
	Mean annual temperature	MT
Temperature-related	Monthly minimum temperature (TME, °C)	TMF.jan, TMF.feb, TMF.mar, TMF.apr, TMF.may, TMF.jun, TMF.jul, TMF.ago, TMF.sep, TMF.oct, TMF.nov, TMF.dec
	Temperature of the coldest month	<ul style="list-style-type: none"> <li>mean temperature of the coldest month (MCMT)</li> <li>average minimum temperature of the coldest month (MINCMT)</li> </ul>
	Monthly maximum temperature (TMC, °C)	TMC.jan, TMC.feb, TMC.mar, TMC.apr, TMC.may, TMC.jun, TMC.jul, TMC.ago, TMC.sep, TMC.oct, TMC.nov, TMC.dec
	Temperature of the warmest month	<ul style="list-style-type: none"> <li>mean temperature of the warmest month (MWMT)</li> <li>average maximum temperature of the warmest month (MAXWMT)</li> </ul>
	Continentality (°C)	TD = MWMT – MCMT
	Growing degree-days with temperature above 5 °C	DD5
Precipitation-related	Frost period (month)	FP
	Annual precipitation (mm)	PREC.annl
	Seasonal precipitation (mm)	PREC.win, PREC.spr, PREC.sum, PREC.son
	Annual heat-moisture index	AHM = MT + 10/(PREC.annl/1000), based upon [10]
	Summer heat-moisture index	SHM = MAXWMT/(PREC.sum/1000), based upon [10]

jan, feb, mar, apr, may, jun, jul, ago, sep, oct, nov, dec are the abbreviations for the months of the year, from January to December. annl means annual. win, spr, sum and aut are the abbreviations for winter, spring, summer and autumn, respectively.

(2) We used the WorldClim climate database [43,44]—the average climate was calculated for the period between 1970 and 2000—at 30 arc sec resolution ( $\sim 1 \times 1$  km), to make spatial predictions of tree height growth for the current and future climates. The climate values for the planting sites and population origins for the current climate were represented by the average climate, as calculated for the period 1970–2000. For future climates, we averaged five global circulation models (GISS-E2-R, HadGEM2-AO, IPSL-CM5A-LR, MIROC-ESM, and NorESM1-M) available in WorldClim [44] for the Representation Concentration Pathway (RCP) 8.5 trajectory for the year 2070. RCPs are greenhouse gas concentration (not emissions) trajectories adopted by the IPCC in the last Assessment Report (AR5) [45]. The RCP 8.5 trajectory is the most aggressive trajectory, and it predicts an increase in the mean temperature of between 2.0 °C and 3.7 °C during the 21st century. Hence, using this scenario for our predictions will show the worst expected outcome. The climate values for the planting sites were represented by the average climate predicted for the year 2070, while the climate values for the populations origins were represented by the average climate of the period 1970–2000.

### 2.3. Selection of Climate Variables

To identify linear and non-linear co-variations between tree height growth and the climate variables, both between the planting sites and at the populations' origins, we used Pearson and Spearman correlation analyses. Based on the correlation results, we set a cutoff of  $\rho \geq |0.5|$  to select the climate variables for the planting sites, and of  $\rho \geq |0.08|$ , to select the climate variables for the populations' origins. For further analyses, all climate variables were standardized: i.e., the mean was subtracted from each value and divided by the standard deviation. We selected 29 climate variables for the planting sites, and five variables for the populations. Climate variables for the planting sites included temperature- and precipitation-related variables, while climate variables for the populations were mostly precipitation-related (Table A1 in Appendix A).

### 2.4. Linear Mixed-Effect Models of Tree Height Growth

We fitted linear mixed-effect models of tree height growth that accounted for both the climate of the planting site and the climate of the population origin [10,12,13]. To build the best supported linear mixed-effect model, we followed two steps:

(1) We fitted a battery of linear mixed-effect models of pairwise combinations between one climate variable of the planting site, and another climate variable of the population origin from the set of previous selected climate variables to find the best combination. These models included the structure of the experimental design in the random part (two random effects, blocks nested into planting sites, and populations), and the linear and quadratic terms; and the linear interaction term of these climate variables in the fixed part [12] (Equation (1)). We selected the model with the lowest Akaike Information Criterion value (AIC) [46].

$$H_{ijk} = \alpha_0 + \alpha_1(\text{clim\_s})_{ik} + \alpha_2(\text{clim\_p})_{ij} + \alpha_3(\text{clim\_s})_{ik}^2 + \alpha_4(\text{clim\_p})_{ij}^2 + \alpha_5(\text{clim\_s})_{ik} \times (\text{clim\_p})_{ij} + \beta_1(\text{Planting.site/Block}) + \beta_2(\text{Population}) + \varepsilon_{ijk}, \quad (1)$$

where  $H_{ijk}$  is tree height growth of the  $i$ th individual of the  $j$ th population in the  $k$ th planting site.  $\alpha_s$  is the set of  $n$  parameters associated with the fixed effects of the model,  $\text{clim\_p}_{ij}$  is the climate at the population of origin of the  $i$ th individual of the  $j$ th population;  $\text{clim\_s}_{ik}$  is the climate at the planting site of the  $i$ th individual in the  $k$ th planting site.  $\beta_s$  are the random effects.  $\varepsilon_{ijk}$  is the residual distribution of the  $i$ th individual of the  $j$ th population in the  $k$ th planting site following a Gaussian distribution.

(2) We built the best supported linear mixed-effect model with the best combination of climate variables selected in the previous step. First, the random part remained invariable, and included the experimental design structure described above (Equation (1)). Second, we defined a full model that included the linear and quadratic terms of both the climate at the planting site and the climate at the population origin, and the linear interaction term of both terms. The model selection of the predictor

variables in the fixed part was conducted by using a hierarchical backward selection procedure. We used the AIC criteria, following the rule that net increments of lower than two units of AIC associated with the elimination of any parameter in the full model determined the exclusion of the parameter from the final model [47,48]. We started with the selection of the two-variable interaction (round 1) and then tested the quadratic effects of both climate variables (rounds 2 & 3) and so on downwards the main effects of each predictor (round 4). Fixed effects were tested, using the maximum likelihood (ML), and random effects were tested using the restricted maximum-likelihood method (REML). We computed the percentage of variance explained by the fixed effects of the best supported model,  $MR^2$ , and the percentage of variance explained by the fixed and random effects together,  $CR^2$ , [49,50]. The goodness-of-fit of the best model was assessed by examining the predicted vs. observed values. We used normal error distribution with an identity link. We used R (version 3.2.3, 10 December 2015) run in the Linux–GNU operating system to perform all of the analyses, and the “lme4” and “lmerTest” packages [50,51].

## 2.5. Assessment of the Local Adaptation of Tree Height Growth for Spanish Scots Pine Populations under the Current Climate

Using the best supported linear mixed-effect model, we calculated for each population the tree height growth at its local environment ( $H_L$ ), and the optimum tree height growth ( $H_{OPT}$ ) attainable at the same environment by a non-local population. To calculate  $H_L$ , we replaced the climatic values of the planting site by those of the population climate of origin (i.e.,  $clim_s = clim_p$ ). The estimation of  $H_{OPT}$  was done in two steps. First, we identified the value of the climate of the population origin, providing the optimum tree height growth ( $CL_{OPT}$ ), using the best supported mixed-effect model. To do that, we calculated the first-order partial derivate of the best supported linear mixed-effect model with respect to the climate variable of the population origin and settled it to zero [14]. Second, we used  $CL_{OPT}$  in our best supported mixed-effect model to obtain  $H_{OPT}$ .

The amount of local adaptation of tree height growth for each population was then calculated as follows:

$$LA_H = H_{OPT} - H_L, \quad (2)$$

A positive value of  $LA_H$  indicates that a non-local population would outperform the local one, suggesting that the local population is not locally adapted. Values of  $LA_H$  that are equal to or close to zero indicate local adaptation. The higher the value of  $LA_H$  is, the higher the degree of maladaptation is.

We computed the climate lags ( $CL_H$ ) for each population associated with  $LA_H$  values, to evaluate the climatic causes of maladaptation; i.e., if the local population does not reach the optimum tree height growth, it could be because it is currently living in a drier or warmer climate (negative values of  $CL_H$ ) or in a wetter or cooler climate (positive values of  $CL_H$ ).

$$CL_H = CL_{OPT} - CL_L, \quad (3)$$

## 2.6. Spatial Predictions of the Local Adaptation of Tree Height Growth for Southern Scots Pine Populations under the Impacts of the Current and Future Climate

We predicted the optimum tree height growth ( $H_{OPT}$ ) and local tree height growth ( $H_L$ ) at age 15, based on our models. Our predictions were performed across the species' range in Spain [52]. Then, we estimated  $LA_H$  as the difference among them. Moreover, we predicted tree height growth by the year 2070 under the RCP 8.5. scenario ( $H_L$ -FUT) [53]. Differences between  $H_L$ -FUT and  $H_L$ , ( $D_{FUT-PRES}$ ), can inform us about the climate change impact on Scots pine populations. Positive values of  $D_{FUT-PRES}$  mean that Scots pine populations will increase the tree height growth, while negative values would indicate a decrease. We used the ‘raster’ package in R for all of the spatial computations.

### 3. Results

#### 3.1. Linear Mixed-Effect Models of Tree Height Growth

First, from the battery of models fitted, the model with the lowest AIC included the spring precipitation of the planting site, *PREC.spr\_s*, and the summer heat moisture index of the population origin, *SHM\_p*, (Table A2). Second, the best supported linear mixed-effect model contained the linear term of the spring precipitation of the planting site, *PREC.spr\_s*, and the linear and quadratic terms of the summer heat moisture index of the population origin, *SHM\_p*, and the linear interaction between *PREC.spr\_s* and *SHM\_p* (Tables 2 and 3). The fixed effects of the model explained 62.36% ( $MR^2$ ) of the variance, and 75.14% ( $CR^2$ ) of the variance was explained by the fixed and random effects together. An examination of the residuals indicated that the main assumptions of linear mixed-effect models were met (Figure A2).

**Table 2.** Fixed effects selection for the tree height growth model, following a hierarchical backward procedure using AIC [46] (see Section 2.4 for a detailed description). d.f.: degrees of freedom, AIC: Akaike values,  $\Delta AIC$ : difference in AIC values between alternative models.  $MR^2$  is the percentage of the variance explained by the fixed effects of the model.  $CR^2$  is the percentage of the variance explained by the fixed and random effects of the model.  $MR^2$  and  $CR^2$  values are given for the best supported mixed-effect model.

Fixed Effect Selection	d.f.	AIC	$\Delta AIC$	$MR^2$	$CR^2$
(Round 1) Two-way interaction					
Tree height growth ~ full model	10	50,802.8	0		
Tree height growth ~ full model minus interaction ( <i>PREC.spr_s</i> × <i>SHM_p</i> )	9	50,824.2	21.44		
* (Round 2) Quadratic effect planting site					
Tree height growth ~ full model	10	50,802.8	0		
Tree height growth ~ full model minus quadratic effect ( <i>PREC.spr_s</i> )	9	50,801.4	−1.31		
* (Round 3) Quadratic effect population					
Tree height growth ~ full model	9	50,801.4	0		
Tree height growth ~ full model minus quadratic effect ( <i>SHM_p</i> )	8	50,804.2	2.77		
* (Round 4) Main effects					
Tree height growth ~ full model	9	50,801.4	0	62.36	75.14
Tree height growth ~ full model minus linear term ( <i>PREC.spr_s</i> )	7	50,835.4	33.94		
Tree height growth ~ full model minus linear term (no <i>SHM_p</i> )	6	50,830.1	28.69		
Tree height growth ~ intercept model	5	50,842.6	41.13		

\* Rounds 2, 3 and 4 of the backward selection began with the best supported model obtained in the previous round. *PREC.spr\_s* is the spring precipitation at the planting site. *SHM\_p* is the summer heat moisture index at the population origin.

The spring precipitation of the planting sites (*PREC.spr\_s*) had a positive effect on tree height growth (Figure 1). The summer heat moisture index (*SHM\_p*) drove the among-population differentiation in the studied populations. Specifically, populations that originated in sites with intermediate values of the summer heat moisture index, *SHM*, displayed the highest tree height growth, while populations that originated in sites with either high or low values of *SHM* presented lower tree height growth. This pattern varied across the *PREC.spr\_s* gradient, due to the interaction term between *PREC.spr\_s* and *SHM\_p* (Table 3 and Figure 1).



**Table 3.** Mean, standard error (SE), *t*-values and *p*-values are given for the fixed effects of the tree height growth model in the first panel; and standard deviation (SD) for the random effects are given in the second panel.

Fixed Effects				
	Mean	SE	<i>t</i> -Value	<i>p</i> -Value
(Intercept)	335.414	19.873	16.878	$1.34 \times 10^{-5}$ ***
PREC.spr_s	124.186	19.189	6.472	$2.96 \times 10^{-3}$ **
SHM_p	−9.091	5.694	−1.597	$1.34 \times 10^{-1}$ n.s.
(SHM_p) <sup>2</sup>	−8.562	3.894	−2.199	$4.64 \times 10^{-2}$ *
PREC.spr_s × SHM_p	−5.794	1.195	−4.848	$1.29 \times 10^{-6}$ ***
Random Effects				
	SD			
Block/Planting site	31.33			
Population	20.2			
Planting site	42.8			
Residual	79.15			

Asterisks indicate statistical significance at a *p*-value of lower than: 0.001 (\*\*\*); 0.01 (\*\*); 0.05 (\*) or 0.1 (.) or 1 (n.s., not significant). PREC.spr\_s is the spring precipitation at the planting site. SHM\_p is the summer heat moisture index at the population origin.

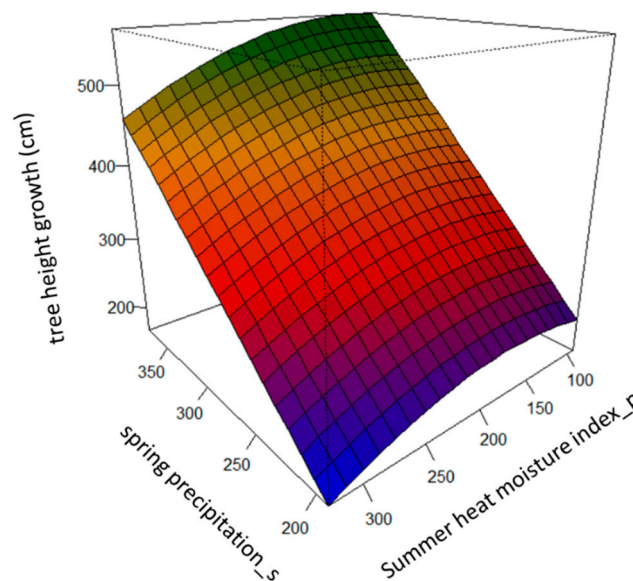


**Figure 1.** Predicted tree height growth (cm), based on the best supported linear mixed-effect model across the gradients of spring precipitation of the planting sites, PREC.spr\_s, and of the summer heat moisture index of the populations' origin, SHM\_p.

### 3.2. Assessment of the Local Adaptation of Tree Height Growth for Spanish Scots Pine Populations under the Current Climate

Most of the populations, except two, underperformed at their local environment, as shown by  $LA_H$  values that were different from zero (Table 4). However, the  $LA_H$  values were small, and they were specifically below 5 cm in 11 out of the 16 populations tested (Table 4). Most of the populations were currently growing under drier conditions, as we found negative values in climatic lags  $CL_H$ . This may prevent the optimum tree height growth from being reached. Two out of the 16 populations were growing under wetter conditions, as we found positive values in  $CL_H$  (Table 4).

**Table 4.** Predictions of local tree height growth,  $H_L$  (cm), and optimum tree height growth,  $H_{OPT}$  (cm), for each population, based upon the best supported model.

Population	PREC.spr_p	CL <sub>L</sub>	H <sub>L</sub> (cm)	CL <sub>OPT</sub>	H <sub>OPT</sub> (cm)	LA <sub>H</sub> (cm)	CL <sub>H</sub>
Baza	265	325.00	239.17	152.34	309.24	70.07	−172.66
Navarredonda de Gredos	237	282.83	229.54	159.87	264.98	35.43	−122.96
Campisábalos	211	239.66	211.75	166.87	224.09	12.34	−72.79
Galve de Sorbe	227	221.77	241.20	162.56	249.22	8.02	−59.21
Morrano	185	205.41	181.13	173.86	183.40	2.27	−31.54
Castell de Cabrés	205	197.74	212.78	168.48	214.68	1.90	−29.26
La Cenia	298	179.43	359.13	143.45	361.79	2.66	−35.98
Navafria	327	175.18	404.95	135.66	408.12	3.17	−39.52
La Granja	377	164.96	485.11	122.21	488.71	3.60	−42.76
Gúdar	202	155.77	209.40	169.30	209.92	0.52	13.53
San Zadornil	267	154.55	312.41	151.80	312.41	0.00	−2.74
Covaleda	327	148.13	407.92	135.66	408.12	0.20	−12.47
Orihuela del Tremedal	297	147.56	360.13	143.73	360.13	0.00	−3.83
Puebla de Lillo	477	118.18	651.63	95.28	652.34	0.70	−22.90
Borau	400	92.37	524.20	116.01	526.11	1.92	23.64
Pobla de Lillet	226	91.69	234.84	162.84	247.59	12.75	71.15

Differences between the optimum and local tree height growth are given in LA<sub>H</sub> (cm). Differences in climate between the optimum and local tree height growth are given in CL<sub>H</sub>. CL<sub>L</sub> refers to values of the climate variable of the summer heat moisture index, SHM, of the population origin. CL<sub>OPT</sub> refers to values of the climate variable of the summer heat moisture index, SHM, where the maximum tree height growth is reached.

### 3.3. Spatial Predictions of the Local Adaptation of Tree Height Growth for Southern Scots Pine Populations under the Impacts of the Current and Future Climate

Most southern Scots pine populations are locally adapted (LA<sub>H</sub> values close to zero) or slightly maladapted (LA<sub>H</sub> values of around 5; gray to light-yellow colors in Figure 2) to current climates. Just a few populations of Scots pine at the southernmost part of the distribution presented large values of LA<sub>H</sub> (yellow to red colors in Figure 2).

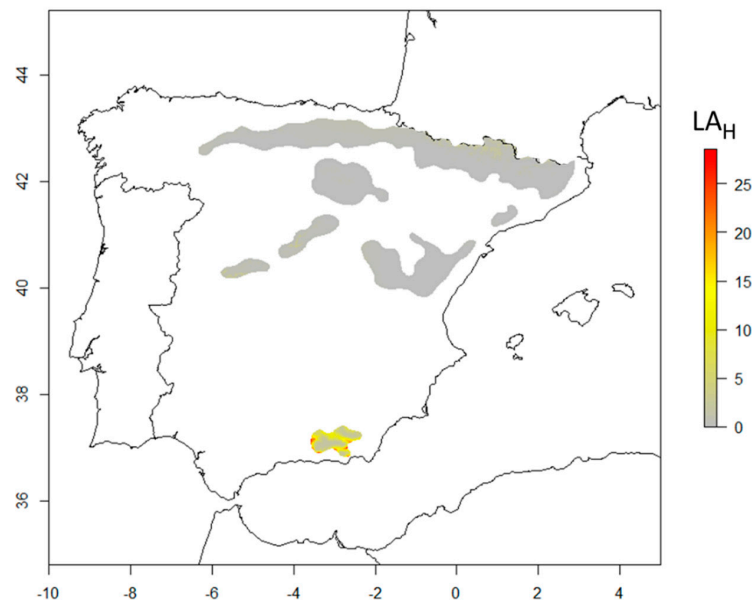


**Figure 2.** Local adaptation of tree height growth to current climate for southern Scots pine populations at 15 years-old (LA<sub>H</sub>, cm) in Spain. LA<sub>H</sub> provides a measurement of the local adaptation in cm. Zero values indicate local adaptation, the rest of the values denote a lack of local adaptation. Gray to light-yellow colors indicate that the populations are locally or slightly maladapted (LA<sub>H</sub> ranges between 0 and 5 cm), whilst yellow to red colors indicate populations maladapted to the current climate (LA<sub>H</sub> > 5 cm).



Our model predicted an increase in tree height growth in year 2070, particularly in the north (Pyrenees), and in high-elevation areas (Figure 3). The model predicted a decrease in tree height growth in the center and in the north-west. Populations at the southernmost part of the distribution were predicted to decrease moderately (Figure 3).

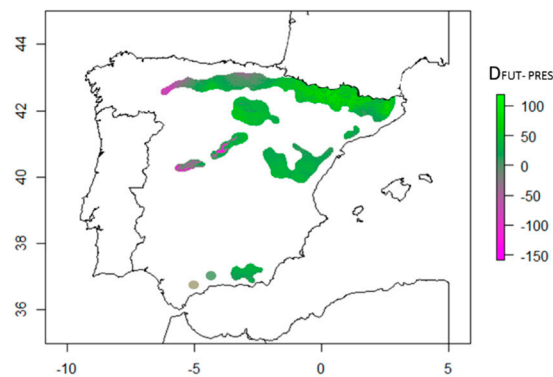


**Figure 3.** Differences in tree height growth predictions ( $D_{FUT-PRES}$ , cm) between future (year 2070, RCP 8.5) and tree height growth for current climate conditions. Violet to gray colors indicate a decrease in tree height predicted for 2070, and gray to green colors indicate an increase in the potential tree height growth, as predicted by the model.

## 4. Discussion

### 4.1. The Main Climatic Drivers Shaping Among-Population Differentiation and Phenotypic Plasticity Responses of Tree Height Growth

The main climatic driver shaping genetic differentiation among the populations, in terms of tree height growth, was the summer moisture index ( $SHM_p$ ), a proxy of drought. This result suggests that drought has probably been a selective factor, which is in agreement with previous studies [39,54]. For instance, our model predicted that populations that originated under more stressful conditions, i.e., with higher values of the summer moisture index calculated for the period of years between 1961 and 1999 (Figure 1), would present a slower rate of growth, which is a suggested strategy for increasing drought adaptation by reducing aboveground biomass [39,55]. Other adaptive responses to reduce cavitation risks, induced either by drought or frost stresses, have been described for the same populations. For example, populations from dry sites show large average tracheid lumen diameters, to assure hydraulic conductivity, whilst populations from sites with frequent freeze–thaw events present small tracheid lumen diameters [53]. Also, it has been suggested that southern populations adapt their leaf conductance and stomata control for less transpiration through the needles [54].

Phenotypic plastic responses were driven by spring precipitation ( $PREC.spr_s$ ). We found a common pattern where tree height growth decreases under drier conditions (Table 3 & Figure 1). This result agrees with the findings of a previous study, where annual precipitation drove phenotypic plastic responses in tree height–diameter allometry for the same species [40]. Now, this study has allowed us to identify that tree height growth is largely driven by the rainfall that falls during the spring season. This could be related to the fact that maximum cambial activity for this species has been described to take place between mid-March and end of August [55], suggesting that Scots pine populations make better use of the rainfall in the early growing season than in the late season (autumn).

Both results highlight that water availability drives the phenotype variations in tree height growth in Scots pine populations, which is consistent with the limiting role that water plays in Mediterranean ecosystems [56].

#### 4.2. Most Southern Scots Pine Populations are Locally Adapted to the Current Climate

The finding of local adaptations for most of the southern Scots pine populations was in agreement with our expectations (Table 4 & Figure 2). One possible explanation could be related to the species' demographic history. During the last glacial maximum, Scots pine had many refuge areas scattered throughout southern Europe [57,58]. These populations may have adapted to the particular conditions of this part of the range during the postglacial migrations [24,33]. Furthermore, the fragmented distribution of the species in the southern part of the range, and the low levels of gene flow among populations might have favored local adaptation [31]. However, we found maladaptation in the southernmost populations (Figure 2). This result could be explained accordingly by the gene flow asymmetry theory across species' ranges [14]: maladapted populations might have received alleles from core and northern populations that are pre-adapted to cooler or wetter conditions than those found at the southernmost part of the range, limiting local adaptation [10,14].

Nevertheless, our findings of local adaptation may change if other fitness-related traits were considered. For instance, fitness-related traits can present trade-offs across the species' ranges [21,23]. Typically, demographic compensation has been found in several marginal populations [21–23]. We could expect the same for Scots pine, given that the southernmost Spanish populations show low early recruitment as a consequence of high seedling mortality, low seed production, and high predation rates [56]. Hence, a wider perspective of Scots pine adaptation patterns using other traits than those related with growth is desirable.

#### 4.3. The Importance of Considering Genetic and Plastic Effects for Evaluating Tree Height Growth for Future Climates

Our predictions should be interpreted as the combination of adaptation and plasticity effects in tree height growth. The contribution of genetic effects to explain tree growth variation in our data was lower than that of phenotypic plasticity, although it was of similar magnitude ( $\Delta AIC = 28.69$  and  $\Delta AIC = 33.94$ , respectively, Table 1). This result highlights that both adaptations to local conditions and the capacity to adjust to the environment through plastic responses are crucial for understanding the performance of Scots pine populations for future climates.

Future predictions for an average tree, showing an increase in tree height, suggest that plasticity can help with tree acclimation to the new climate, and it can then compensate for the imprint of local adaptation, which is a common characteristic in trees [57]. Our results are partially in agreement with [27], where moderate increases in tree growth for Scots pine populations are predicted in Spain under the RCP 8.5 scenario for 2050, although tree growth does decrease, especially in southern low-elevation sites, in 2070. In the northern and high-elevation areas (Pyrenees), warmer conditions would benefit tree growth by lengthening the growing season, thus increasing net photosynthesis, stomatal conductance, and specific hydraulic conductivity [58]. However, opposite results of tree growth decrease have been reported for this species in Spain [35,59], as lower precipitation regimes combined with higher temperatures would presumably lead to a general pattern of more frequent drought events, higher evapotranspiration, and reduced soil water availability in the future. However, none of these studies have accounted for the plasticity capacity of the species, and this could explain the differences in the forecasts. Moreover, few populations in the north-west and in the central part of the species distribution in Spain have been predicted to decrease in tree height growth. This prediction could be reflected by the sharp decrease in spring precipitation that is expected for year 2070 (RCP 8.5.) in these areas (Figure A3). Our forecast could be related to site characteristics (such as soil depth, nutrient availability, geomorphological features, etc.) that can make water availability difficult.

Finally, caution is needed when interpreting our predictions beyond the year 2070, as we do not know whether plasticity will help with acclimation to new environments in the far future, and evolutionary adaptation may then become necessary. Contrary to our expectations, in terms of the species' growth, the forecast for southern Scots pine populations is generally favorable. Nonetheless, our results are based on common gardens. In natural populations, other factors, such as above-

and below-ground competition, herbivory, management practices, etc., can strongly modify our expectations of Scots pine growth and adaptation to climate change.

## 5. Conclusions

Most of the populations of Scots pine in Spain were locally adapted to drought. This result suggests that marginal populations, despite inhabiting limiting environments, can become adapted to their current local conditions. In addition, the local adaptation and acclimation capacity of populations can help marginal populations to keep pace with climate change. Our results highlight the importance of analyzing populations' capacity to cope with climate change, on a case-by-case basis.

**Author Contributions:** In the present study, the authors contributed to the different sections as follows: Conceptualization, N.V.-P. and M.B.G.; methodology, N.V.-P., N.G.-M. and M.B.G.; formal analysis, N.V.-P.; manuscript writing—original draft preparation N.V.-P., N.G.-M., and M.B.G.; writing—review and editing N.V.-P., S.C.G.-M., R.A., M.B.G.

**Funding:** This study was funded by: the Spanish Ministry of Economy and Competitiveness, through the following projects VULPINECLIM (MINECO, CGL2013-44553-R), ADAPCON (CGL2011-30182-C02-01), FENOPIN (AGL2012-40151-C03-02), and the following two projects: “Investments for the future” Programme IdEx Bordeaux (reference ANR-10-IDEX-03-02) and the EFPA (Département Ecologie des Forêts, Prairies et milieux Aquatiques) INRA (Institut National de la Recherche Agronomique) Integration Project. NVP was funded by a fellowship FPI-MCI (BES-2009-025151) and a postdoctoral contract associated with the European Project H2020 “Optimising the management and sustainable use of forest genetic resources in Europe” (GenTree; grant agreement No 676876). NGM was supported by an AgreenSkills postdoctoral fellowship. The data is part of the Spanish Network of Genetic Trials (GENFORÉD), and it is publicly available upon request through [www.genfored.es](http://www.genfored.es).

**Acknowledgments:** We acknowledge the GENFORÉD team: F. del Caño, E.D. Barba, F.J. Auñón, and M.R. Chambel—who measured, gathered, and stored the data used in this research article.

**Conflicts of Interest:** The authors declare no conflict of interest.

## Appendix A

**Table A1.** Pearson and Spearman correlation coefficients between climate data, at the planting sites and at the population origin, and tree height growth of Scots pine from 15-year-old.

Climate at the Planting Site			Climate at the Population Origin		
Variables	Pearson	Spearman	Variables	Pearson	Spearman
TMF.jan	−0.565	−0.384	TMF.jan	0.025	0.019
TMF.feb	−0.581	−0.497	TMF.feb	0.006	0
TMF.mar	−0.62	−0.554	TMF.mar	0.007	−0.002
TMF.apr	−0.65	−0.616	TMF.apr	0.004	−0.004
TMF.may	−0.371	−0.382	TMF.may	−0.007	−0.01
TMF.jun	−0.055	−0.111	TMF.jun	−0.002	0.003
TMF.jul	−0.107	−0.038	TMF.jul	−0.016	−0.025
TMF.ago	−0.171	0.009	TMF.ago	−0.021	−0.036
TMF.sep	−0.534	−0.536	TMF.sep	−0.014	−0.029
TMF.oct	−0.633	−0.554	TMF.oct	0.005	−0.009
TMF.nov	−0.636	−0.594	TMF.nov	0.01	0.006
TMF.dec	−0.577	−0.479	TMF.dec	0.024	0.01
TMC.jan	−0.32	−0.174	TMC.jan	−0.017	−0.031
TMC.feb	−0.478	−0.47	TMC.feb	−0.03	−0.023
TMC.mar	−0.628	−0.644	TMC.mar	−0.043	−0.039
TMC.apr	−0.648	−0.644	TMC.apr	−0.034	−0.037
TMC.may	−0.607	−0.695	TMC.may	−0.055	−0.057
TMC.jun	−0.469	−0.345	TMC.jun	−0.055	−0.064
TMC.jul	−0.494	−0.478	TMC.jul	−0.075	−0.087
TMC.ago	−0.379	−0.378	TMC.ago	−0.075	−0.086
TMC.sep	−0.438	−0.44	TMC.sep	−0.077	−0.086

Table A1. Cont.

Climate at the Planting Site			Climate at the Population Origin		
Variables	Pearson	Spearman	Variables	Pearson	Spearman
TMC.oct	−0.443	−0.521	TMC.oct	−0.034	−0.024
TMC.nov	−0.269	−0.208	TMC.nov	−0.028	−0.027
TMC.dec	−0.287	−0.174	TMC.dec	−0.016	−0.014
T.jan	−0.457	−0.407	T.jan	0.003	0
T.feb	−0.569	−0.497	T.feb	−0.014	−0.018
T.mar	−0.66	−0.684	T.mar	−0.023	−0.022
T.apr	−0.648	−0.616	T.apr	−0.019	−0.027
T.may	−0.586	−0.616	T.may	−0.034	−0.037
T.jun	−0.337	−0.345	T.jun	−0.03	−0.029
T.jul	−0.358	−0.282	T.jul	−0.048	−0.052
T.ago	−0.311	−0.378	T.ago	−0.051	−0.049
T.sep	−0.492	−0.378	T.sep	−0.05	−0.042
T.oct	−0.534	−0.521	T.oct	−0.016	−0.027
T.nov	−0.466	−0.521	T.nov	−0.011	−0.023
T.dec	−0.426	−0.407	T.dec	0.001	−0.006
PREC.annl	0.675	0.663	PREC.ann	0.073	0.105
PREC.win	0.575	0.516	PREC.win	0.035	0.038
PREC.spr	0.779	0.663	PREC.spr	0.073	0.088
PREC.sum	0.609	0.497	PREC.sum	0.08	0.079
PREC.son	0.611	0.487	PREC.son	0.079	0.107
MT	−0.544	−0.458	MT	−0.024	−0.031
MCMT	−0.262	−0.282	MCMT	−0.056	−0.057
MAXWMT	−0.416	−0.378	MAXWMT	−0.072	−0.083
MCMT	−0.446	−0.407	MCMT	0.01	0.007
MINCMT	−0.561	−0.351	MINCMT	0.031	0.027
FP	0.651	0.594	FP	−0.016	0.009
DD5	−0.613	−0.548	DD5	−0.004	−0.012
TD	0.282	0.33	TD	−0.103	−0.107
AHM	−0.611	−0.663	AHM	−0.083	−0.087
SHM	−0.376	−0.554	SHM	−0.108	−0.103

T.#, TMC.# and TMF.# mean minimum, maximum and mean average monthly (#) temperatures (°C); PREC.ann means annual precipitation (mm); PREC.win, PREC.spr, PREC.sum, PREC.aut, for winter, spring, summer and autumn, respectively; TM means mean annual temperature (°C); MINCMT means mean of the minimum temperatures from the coldest month (°C); FP means frost period (month); DD5 means degree days-period over 5 °C; TD means continentality; AHM means annual heat moisture index; and SHM means summer heat moisture index.

**Table A2.** AIC values from the battery of linear-mixed effect models fitted. Climate variables of the planting sites are specified with \_s and climate at the populations' origin with \_p. The best supported model showed the lowest AIC and it is highlighted with bold.

	PREC.ann_p	PREC.sum_p	PREC.aut_p	TD_p	SHM_p
TMF.jan_s	49,559.63	49,551.74	49,554.15	49,557.09	49,546.44
TMF.feb_s	49,560.72	49,551.38	49,555.08	49,557.30	49,547.21
TMF.mar_s	49,560.71	49,550.99	49,555.01	49,557.11	49,546.92
TMF.apr_s	49,560.68	49,551.40	49,555.01	49,557.05	49,546.58
TMF.sep_s	49,559.38	49,550.93	49,554.04	49,557.11	49,546.46
TMF.ocT_s	49,560.05	49,550.89	49,554.45	49,556.87	49,546.21
TMF.nov_s	49,560.59	49,550.80	49,554.90	49,557.00	49,546.73
TMF.dec_s	49,558.35	49,551.16	49,553.06	49,556.43	49,545.56
TMC.mar_s	49,559.41	49,551.82	49,553.99	49,556.32	49,545.58
TMC.apr_s	49,560.07	49,551.58	49,554.50	49,556.48	49,545.95
TMC.may_s	49,558.67	49,550.63	49,553.19	49,555.64	49,544.68
TMC.ocT_s	49,560.10	49,551.94	49,554.42	49,557.14	49,546.54
T.feb_s	49,560.11	49,551.59	49,554.50	49,557.14	49,546.43

Table A2. Cont.

	PREC.ann_p	PREC.sum_p	PREC.aut_p	TD_p	SHM_p
T.mar_s	49,559.29	49,550.86	49,553.77	49,556.02	49,545.26
T.abr_s	49,560.58	49,551.67	49,554.94	49,556.90	49,546.43
T.may_s	49,559.93	49,551.30	49,554.34	49,556.65	49,545.82
T.ocT_s	49,560.85	49,552.14	49,555.19	49,557.78	49,547.12
T.nov_s	49,560.74	49,552.16	49,554.99	49,557.50	49,547.12
PREC.ann_s	49,556.66	49,547.51	49,551.56	49,554.96	49,542.98
PREC.win_s	49,557.89	49,548.82	49,553.03	49,557.20	49,544.34
PREC.spr_s	49,551.91	49,542.89	49,546.79	49,549.92	<b>49,537.76</b>
PREC.sum_s	49,559.40	49,550.01	49,553.93	49,556.48	49,545.86
PREC.aut_s	49,558.02	49,548.82	49,552.83	49,555.99	49,544.56
TM_s	49,560.08	49,551.91	49,554.55	49,557.53	49,546.59
MINCMT_s	49,559.40	49,551.46	49,553.88	49,556.69	49,546.14
FP_s	49,559.60	49,550.39	49,553.99	49,556.29	49,545.69
DD5_s	49,559.15	49,550.99	49,553.67	49,556.52	49,545.53
AHM_s	49,553.34	49,546.99	49,548.73	49,553.97	49,541.36
SHM_s	49,557.06	49,551.09	49,551.97	49,556.55	49,545.83

T.#, TMC.# and TMF.# mean minimum, maximum and mean average monthly (#) temperatures (°C); PREC.ann means annual precipitation (mm); PREC.win, PREC.spr, PREC.sum, PREC.aut, for winter, spring, summer and autumn, respectively; TM means mean annual temperature (°C); MINCMT means mean of the minimum temperatures from the coldest month (°C); FP means frost period (month); DD5 means degree days-period over 5 °C; TD means continentality; AHM means annual heat moisture index; and SHM means summer heat moisture index.

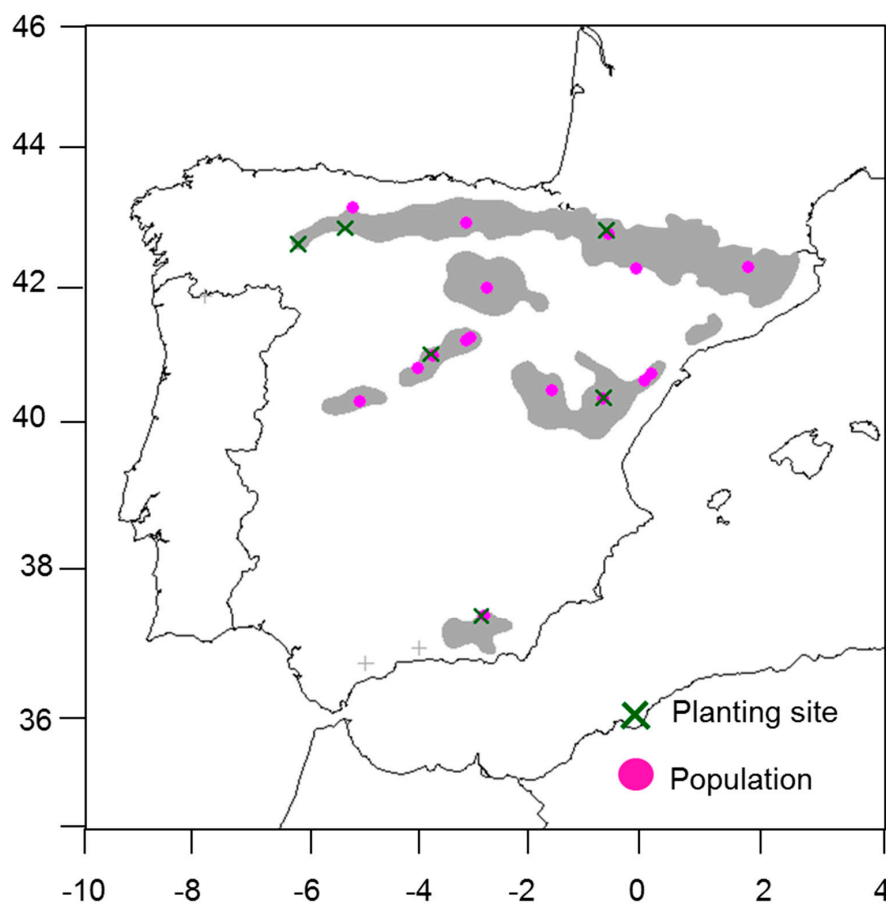


**Figure A1.** Network of provenance common gardens in Spain (GENFORED): Planting sites (green crosses), populations (pink circles). The species distribution range is shown in gray (two isolated populations are represented by “+” in gray).

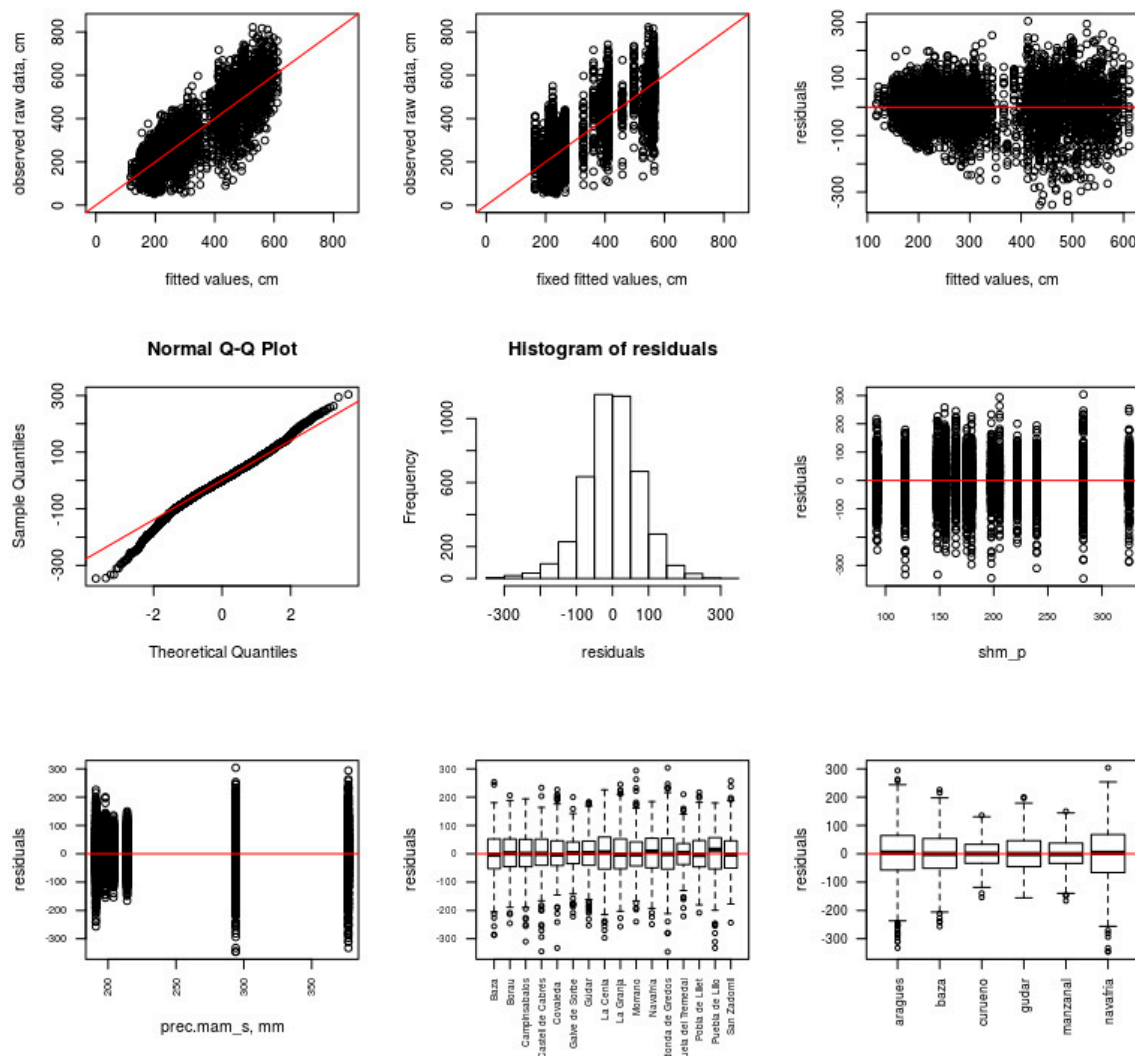


**Figure A2.** Graphical summary of the best supported model for Scots pine populations from 15 year-old. Top line, left to right: plot of observed raw data vs. predicted; plot of observed raw data vs. predicted data; residuals vs. predicted data. Middle line: qq-plot; histogram of residuals values; residuals vs. shm\_p (summer heat moisture index). Bottom line: residuals vs. prec.mam\_s (spring precipitation); residuals vs. population factor; residuals vs. planting site factor.



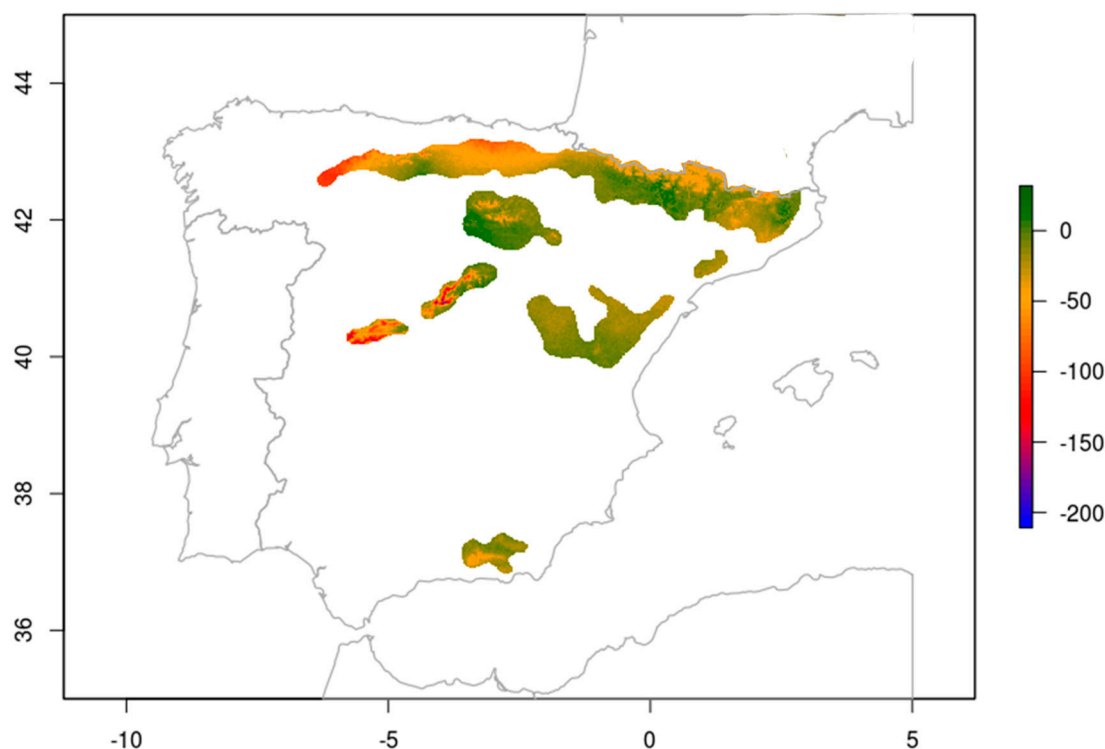


**Figure A3.** Spring precipitation anomaly between year 2070 (RCP 8.5) and current climate (baseline: average climate calculated for the period 1970–2000).

## References

1. Lindner, M.; Maroschek, M.; Netherer, S.; Kremer, A.; Barbati, A.; Garcia-Gonzalo, J.; Seidl, R.; Delzon, S.; Corona, P.; Kolström, M.; et al. Climate change impacts, adaptive capacity, and vulnerability of European forest ecosystems. *For. Ecol. Manag.* **2010**, *259*, 698–709. [[CrossRef](#)]
2. Pretzsch, H.; Biber, P.; Schütze, G.; Uhl, E.; Rötzer, T. Forest stand growth dynamics in Central Europe have accelerated since 1870. *Nat. Commun.* **2014**, *5*, 4967. [[CrossRef](#)] [[PubMed](#)]
3. McMahon, S.M.; Parker, G.G.; Miller, D.R. Evidence for a recent increase in forest growth. *Proc. Natl. Acad. Sci. USA* **2010**, *107*, 3611–3615. [[CrossRef](#)] [[PubMed](#)]
4. Machar, I.; Vlckova, V.; Bucek, A.; Vozenilek, V.; Salek, L.; Jerabkova, L.; Machar, I.; Vlckova, V.; Bucek, A.; Vozenilek, V.; et al. Modelling of Climate Conditions in Forest Vegetation Zones as a Support Tool for Forest Management Strategy in European Beech Dominated Forests. *Forests* **2017**, *8*, 82. [[CrossRef](#)]
5. Allen, C.D.; Macalady, A.K.; Chenchouni, H.; Bachelet, D.; McDowell, N.; Vennetier, M.; Kitzberger, T.; Rigling, A.; Breshears, D.D.; Hogg, E.H.; et al. A global overview of drought and heat-induced tree mortality reveals emerging climate change risks for forests. *For. Ecol. Manag.* **2010**, *259*, 660–684. [[CrossRef](#)]
6. Lévesque, M.; Siegwolf, R.; Saurer, M.; Eilmann, B.; Rigling, A. Increased water-use efficiency does not lead to enhanced tree growth under xeric and mesic conditions. *New Phytol.* **2014**, *203*, 94–109. [[CrossRef](#)]
7. Gómez-Aparicio, L.; García-Valdés, R.; Ruiz-Benito, P.; Zavala, M.A. Disentangling the relative importance of climate, size and competition on tree growth in Iberian forests: Implications for forest management under global change. *Glob. Chang. Biol.* **2011**, *17*, 2400–2414. [[CrossRef](#)]
8. Kunstler, G.; Falster, D.; Coomes, D.A.; Hui, F.; Kooyman, R.M.; Laughlin, D.C.; Poorter, L.; Vanderwel, M.; Vieilledent, G.; Wright, S.J.; et al. Plant functional traits have globally consistent effects on competition. *Nature* **2016**, *529*, 204–207.
9. Cornelius, J. Heritabilities and additive genetic coefficients of variation in forest trees. *Can. J. For. Res.* **1994**, *24*, 372–379. [[CrossRef](#)]
10. Leites, L.P.; Robinson, A.P.; Rehfeldt, G.E.; Marshall, J.D.; Crookston, N.L. Height-growth response to climatic changes differs among populations of Douglas-fir: A novel analysis of historic data. *Ecol. Appl.* **2012**, *22*, 154–165. [[CrossRef](#)]

11. Rehfeldt, G.; Ying, C.; Spittlehouse, D.; Hamilton, D. Genetic responses to climate in *Pinus contorta*: Niche breadth, climate change, and reforestation. *Ecol. Monogr.* **1999**, *69*, 375–407. [[CrossRef](#)]
12. Gárate-Escamilla, H.; Hampe, A.; Vizcaíno-Palomar, N.; Robson, T.M.; Benito Garzón, M. Range-wide variation in local adaptation and phenotypic plasticity of fitness-related traits in *Fagus sylvatica* and their implications under climate change. *Glob. Ecol. Biogeogr.* **2019**. [[CrossRef](#)]
13. Vizcaíno-Palomar, N.; Ibáñez, I.; González-Martínez, S.C.; Zavala, M.A.; Alía, R. Adaptation and plasticity in aboveground allometry variation of four pine species along environmental gradients. *Ecol. Evol.* **2016**, *6*, 7561–7573. [[CrossRef](#)]
14. Wang, T.; O'Neill, G.A.; Aitken, S.N. Integrating environmental and genetic effects to predict responses of tree populations to climate. *Ecol. Appl.* **2010**, *20*, 153–163. [[CrossRef](#)] [[PubMed](#)]
15. Savolainen, O.; Pyhäjärvi, T.; Knürr, T. Gene flow and local adaptation in trees. *Annu. Rev. Ecol. Evol. Syst.* **2007**, *38*, 595–619. [[CrossRef](#)]
16. Kawecki, T.J.; Ebert, D. Conceptual issues in local adaptation. *Ecol. Lett.* **2004**, *7*, 1225–1241. [[CrossRef](#)]
17. Hampe, A.; Petit, R.J. Conserving biodiversity under climate change: The rear edge matters. *Ecol. Lett.* **2005**, *8*, 461–467. [[CrossRef](#)]
18. Martínez-Meyer, E.; Díaz-Porras, D.; Peterson, A.T.; Yáñez-Arenas, C. Ecological niche structure and range wide abundance patterns of species. *Biol. Lett.* **2012**, *9*, 20120637. [[CrossRef](#)]
19. Purves, D.W. The demography of range boundaries versus range cores in eastern US tree species. *Proc. R. Soc. B Biol. Sci.* **2009**, *276*, 1477–1484. [[CrossRef](#)]
20. Pedlar, J.H.; McKenney, D.W.; Parra, J.; Jones, P.; Jarvis, A. Assessing the anticipated growth response of northern conifer populations to a warming climate. *Sci. Rep.* **2017**, *7*, 43881. [[CrossRef](#)]
21. Doak, D.F.; Morris, W.F. Demographic compensation and tipping points in climate-induced range shifts. *Nature* **2010**, *467*, 959–962. [[CrossRef](#)] [[PubMed](#)]
22. Benito Garzón, M.; Ruiz-Benito, P.; Zavala, M.A. Interspecific differences in tree growth and mortality responses to environmental drivers determine potential species distributional limits in Iberian forests. *Glob. Ecol. Biogeogr.* **2013**, *22*, 1141–1151. [[CrossRef](#)]
23. Peterson, M.L.; Doak, D.F.; Morris, W.F. Both life-history plasticity and local adaptation will shape range-wide responses to climate warming in the tundra plant *Silene Acaulis*. *Glob. Chang. Biol.* **2018**, *24*, 1614–1625. [[CrossRef](#)] [[PubMed](#)]
24. Morgenstern, E.K. *Geographic Variation in Forest Trees: Genetic Basis and Application of Knowledge in Silviculture*; University of British Columbia: Vancouver, BC, Canada, 1996.
25. Eckenwalder, J.E. *Conifers of the World: The Complete Reference*; Timber Press: Portland, OR, USA, 2009; ISBN 0881929743.
26. Sánchez-Salguero, R.; Camarero, J.J.; Hevia, A.; Madrigal-González, J.; Linares, J.C.; Ballesteros-Cánovas, J.A.; Sánchez-Miranda, A.; Alfaro-Sánchez, R.; Sangüesa-Barreda, G.; Galván, J.D.; et al. What drives growth of Scots pine in continental Mediterranean climates: Drought, low temperatures or both? *Agric. For. Meteorol.* **2015**, *206*, 151–162. [[CrossRef](#)]
27. Sánchez-Salguero, R.; Camarero, J.J.; Gutiérrez, E.; González Rouco, F.; Gazol, A.; Sangüesa-Barreda, G.; Andreu-Hayles, L.; Linares, J.C.; Seftigen, K. Assessing forest vulnerability to climate warming using a process-based model of tree growth: Bad prospects for rear-edges. *Glob. Chang. Biol.* **2017**, *23*, 2705–2719. [[CrossRef](#)] [[PubMed](#)]
28. Kujala, S.T.; Savolainen, O. Sequence variation patterns along a latitudinal cline in Scots pine (*Pinus sylvestris*): Signs of clinal adaptation? *Tree Genet. Genomes* **2012**, *8*, 1451–1467. [[CrossRef](#)]
29. Soranzo, N.; Alía, R.; Provan, J.; Powell, W. Patterns of variation at a mitochondrial sequence-tagged-site locus provides new insights into the postglacial history of European *Pinus sylvestris* populations. *Mol. Ecol.* **2000**, *9*, 1205–1211. [[CrossRef](#)] [[PubMed](#)]
30. Robledo-Arnuncio, J.J.; Collada, C.; Alía, R.; Gil, L. Genetic structure of montane isolates of *Pinus sylvestris* L. in a Mediterranean refugial area. *J. Biogeogr.* **2005**, *32*, 595–605. [[CrossRef](#)]
31. Prus-Glowacki, W.; Stephan, B.R.; Bujas, E.; Alía, R.; Marciniak, A. Genetic differentiation of autochthonous populations of *Pinus sylvestris* (*Pinaceae*) from the Iberian Peninsula. *Plant Syst. Evol.* **2003**, *239*, 55–66. [[CrossRef](#)]

32. Nahal, I. The Mediterranean climate from a biological viewpoint. In *Ecosystems of the World 11: Mediterranean-Type Shrublands*; Di Castri, F., Goodall, W., Specht, R.L., Eds.; Elsevier Scientific Publishing Co.: Amsterdam, The Netherlands, 1981; pp. 63–86.
33. Sánchez-Salguero, R.; Navarro-Cerrillo, R.M.; Camarero, J.J.; Fernández-Cancio, Á. Selective drought-induced decline of pine species in southeastern Spain. *Clim. Chang.* **2012**, *113*, 767–785. [[CrossRef](#)]
34. Castro, J.; Zamora, R.; Hódar, A.J.; Gómez, J. Seedling establishment of a boreal tree species (*Pinus sylvestris*) at its southernmost distribution limit: Consequences of being in a marginal Mediterranean habitat. *J. Ecol.* **2004**, *92*, 266–277. [[CrossRef](#)]
35. Herrero, A.; Rigling, A.; Zamora, R. Varying climate sensitivity at the dry distribution edge of *Pinus sylvestris* and *P. nigra*. *For. Ecol. Manag.* **2013**, *308*, 50–61. [[CrossRef](#)]
36. McDowell, N.; Pockman, W.T.; Allen, C.D.; Breshears, D.D.; Cobb, N.; Kolb, T.; Plaut, J.; Sperry, J.; West, A.; Williams, D.G.; et al. Mechanisms of plant survival and mortality during drought: Why do some plants survive while others succumb to drought? *New Phytol.* **2008**, *178*, 719–739. [[CrossRef](#)] [[PubMed](#)]
37. Falster, D.S.; Westoby, M. Plant height and evolutionary games. *Trends Ecol. Evol.* **2003**, *18*, 337–343. [[CrossRef](#)]
38. Moles, A.T.; Leishman, M.R. The seedling as part of a plant's life history strategy. In *Seedling Ecology and Evolution*; Leck, A., Parker, V.T., Simpson, R.L., Eds.; Cambridge University Press: Cambridge, UK, 2008; pp. 217–238.
39. Alía, R.; Moro, J.; Notivol, E.; Moro-Serrano, J. Genetic variability of Scots pine (*Pinus sylvestris* L.) provenances in Spain: Growth traits and survival. *Silva Fenn.* **2001**, *35*, 27–38. [[CrossRef](#)]
40. Agúndez, D.; Alía, R.; Diez, R. Variación de *Pinus sylvestris* en España: Características de piñas y piñones. *Investig. Agrar. Sist. Recur. For.* **1992**, *1*, 151–162.
41. González-Martínez, S.C.; Burczyk, J.; Nathan, R.; Nanos, N.; Gil, L.; Alía, R. Effective gene dispersal and female reproductive success in Mediterranean maritime pine (*Pinus pinaster* Aiton). *Mol. Ecol.* **2006**, *15*, 4577–4588. [[CrossRef](#)]
42. Gonzalo-Jiménez, J. *Diagnosis Fitoclimática de la España Peninsular Hacia un Modelo de Clasificación Funcional de la Vegetación y de los Ecosistemas Peninsulares Españoles*; Organismo Autónomo Parques Nacionales: Madrid, Spain, 2010; ISBN 978-84-8014-787-3.
43. Fick, S.E.; Hijmans, R.J. WorldClim 2: New 1-km spatial resolution climate surfaces for global land areas. *Int. J. Climatol.* **2017**, *37*, 4302–4315. [[CrossRef](#)]
44. Hijmans, R.J.; Cameron, S.E.; Parra, J.L.; Jones, P.G.; Jarvis, A. Very high resolution interpolated climate surfaces for global land areas. *Int. J. Climatol.* **2005**, *25*, 1965–1978. [[CrossRef](#)]
45. IPCC Climate Change. *Synthesis Report. Contribution of Working Groups I, II and III to the Fifth Assessment Report of the Intergovernmental Panel on Climate Change*; Pachauri, R.K., Meyer, L.A., Eds.; IPCC: Geneva, Switzerland, 2014; p. 151.
46. Akaike, H. Information theory and an extension of the maximum likelihood principle. In *Breakthroughs in Statistics*; Kotz, S., Johnson, N., Eds.; Springer-Verlag: London, UK, 1992; pp. 610–624.
47. Zuur, A.F.; Ieno, E.N.; Walker, N.; Saveliev, A.A.; Smith, G.M. *Mixed Effects Models and Extensions in Ecology with R*; Springer: Berlin/Heidelberg, Germany, 2009; ISBN 978-0-387-87458-6.
48. Bolker, B.M.; Brooks, M.E.; Clark, C.J.; Geange, S.W.; Poulsen, J.R.; Stevens, M.H.H.; White, J.-S.S. Generalized linear mixed models: A practical guide for ecology and evolution. *Trends Ecol. Evol.* **2009**, *24*, 127–135. [[CrossRef](#)]
49. Nakagawa, S.; Schielzeth, H. A general and simple method for obtaining  $R^2$  from generalized linear mixed-effects models. *Methods Ecol. Evol.* **2013**, *4*, 133–142. [[CrossRef](#)]
50. Bates, D.; Maechler, M.; Bolker, B.; Walker, S. Fitting Linear Mixed-Effects Models Using lme4. *J. Stat. Softw.* **2015**, *67*, 1–48. [[CrossRef](#)]
51. Kuznetsova, A.; Brockhoff, P.B.; Rune, H.B. lmerTest Package: Tests in Linear Mixed Effects Models. *J. Stat. Softw.* **2017**, *82*, 1–26. [[CrossRef](#)]
52. Caudullo, G.; Welk, E.; San-Miguel-Ayanz, J. Chorological maps for the main European woody species. *Data Br.* **2017**, *12*, 662–666. [[CrossRef](#)] [[PubMed](#)]
53. Van Vuuren, D.P.; Edmonds, J.; Kainuma, M.; Riahi, K.; Thomson, A.; Hibbard, K.; Hurtt, G.C.; Kram, T.; Krey, V.; Lamarque, J.-F.; et al. The representative concentration pathways: An overview. *Clim. Chang.* **2011**, *109*, 5–31. [[CrossRef](#)]

54. Agúndez, D.; Alía, R.; Stephan, R.; Gil, L.; Pardos, J.A. Ensayo de Procedencias Españolas y Alemanas de *Pinus Sylvestris* L.: Comportamiento en Vivero y Supervivencia en Monte. *Ecología* **1994**, *8*, 245–257.
55. Valladares, F.; Gianoli, E.; Gómez, J.M. Ecological limits to plant phenotypic plasticity. *New Phytol.* **2007**, *176*, 749–763. [[CrossRef](#)] [[PubMed](#)]
56. Castro, J.; Gómez, J.M.; García, D.; Zamora, R.; Hódar, J.A. Seed predation and dispersal in relict Scots pine forests in southern Spain. *Plant Ecol.* **1999**, *145*, 115–123. [[CrossRef](#)]
57. Benito Garzón, M.; Robson, T.M.; Hampe, A.  $\Delta$ Trait SDMs: Species distribution models that account for local adaptation and phenotypic plasticity. *New Phytol.* **2019**, *222*, 1757–1765. [[CrossRef](#)]
58. Choat, B.; Jansen, S.; Brodribb, T.; Cochard, H.; Delzon, S.; Bhaskar, R.; Bucci, S.; Feild, T.; Gleason, S.; Hacke, U.; et al. Global convergence in the vulnerability of forests to drought. *Nature* **2012**, *491*, 752–755. [[CrossRef](#)]
59. Gea-Izquierdo, G.; Montes, F.; Gavilán, R.G.; Cañellas, I.; Rubio, A. Is this the end? Dynamics of a relict stand from pervasively deforested ancient Iberian pine forests. *Eur. J. For. Res.* **2015**, *134*, 525–536. [[CrossRef](#)]



© 2019 by the authors. Licensee MDPI, Basel, Switzerland. This article is an open access article distributed under the terms and conditions of the Creative Commons Attribution (CC BY) license (<http://creativecommons.org/licenses/by/4.0/>).